S36-023

Chlorophyll fluorescence imaging of tobamovirus-infected plants

ML Pérez-Bueno[1], M Ciscato[2], M vandeVen[2], I García-Luque[3], M Barón[1], R Valcke[2]

[1] *Dept. Biochemistry, Cell and Molecular Biology of Plants, Estación Experimental del Zaidín (EEZ, CSIC), E-18008 Granada, Spain. mbaron@eez.csic.es*

[2] *Laboratory of Botany, Dept. SBG, Limburgs Universitair Centrum, Universitaire Campus, B-3590 Diepenbeek, Belgium. Fax: +32-11-268301. roland.valcke@luc.ac.be*

[3] *Dept. Plant Biology, Centro de Investigaciones Biológicas (CIB, CSIC), E-28006 Madrid, Spain. igarcia@cib.csic.es.*

Keywords: fluorescence imaging, PSII, biotic stress, tobamovirus.

Introduction

Some plant stress factors don't alter the homogeneous pattern of photosynthetic efficiency, whereas others induced heterogeneous patterns of leaf photosynthesis. Imaging of chlorophyll (Chl) fluorescence allows quantitative monitoring of its spatial and temporal changes (Lichtenthaler, 1996). This technique has been used for the presymptomatic detection of biotic stress, induced by various pathogens, virus (Balachandran, 1997) and fungi (Peterson and Aylor, 1995; Scholes and Rolfe, 1996).

We have studied a compatible host-pathogen interaction, *Nicotiana benthamiana* plants infected by the Italian strain of the tobamovirus pepper mild mottle virus (PMMoV-I). In a previous work we have shown that this virus induces an inhibition of PSII electron transport, disturbing its donor side. In addition, point data measurements of modulated Chl fluorescence demonstrated a reduction in the efficiency of excitation capture in PSII, probably originating in the thermal dissipation of excess energy (Rahoutei *et al.*, 2000).

To map photosynthesis in infected-leaves, we use in the present work a new red-fluorescence imaging system (Ciscato, 2000) to obtain images corresponding to the quantum yield of PSII (Φ_{PSII}) and the non-photochemical quenching (NPQ), related to energy dissipation.

Material and Methods

Nicotiana benthamiana plants were inoculated in the 3 lower leaves at the 5-6 fully-expanded leaf stage with PMMoV-I. Symptoms start to show up at 5-7 days post-inoculation (d.p.i.). Leaves developed after inoculation (symptomatic leaves) show a severe curling; in contrast, no symptoms were observed in those leaves that were fully expanded at the infection time (asymptomatic leaves). After 14 d.p.i. stunting of the plant was evident.

Red fluorescence imaging by the saturation pulse mode. Samples were dark adapted for 1h and then illuminated by continuous blue actinic light ($200\mu Em^{-2}s^{-1}$) and saturating pulses ($1000\mu Em^{-2}s^{-1}$) at 1, 2, 5, 10, 20, 30, 60, 90, 120, 180, 240 and 300 s. A black & white CCD (equipped with a red cut-off filter, λ= 680 nm) captured images during the application of the first saturating pulse of light (F_M), 1s before (F) and during every pulse (F'_M) in the light-

adapted state. From the processed images, the parameters NPQ (non-photochemical quenching) and Φ_{PSII} (PSII quantum yield) were calculated.

$$\Phi_{PSII} = (F'_M - F)/F'_M \qquad NPQ = (F_M - F'_M)/F'_M$$

Four different experiments with 10 control and 10 virus-infected plants were carried out, imaging 5 symptomatic and 5 asymptomatic leaves. Equivalent young and mature leaves of healthy plants were also investigated.

As an additional step in the imaging analysis, 4 regions of interest (ROIs) of 10x10 pixels were selected in a serie of images of control and infected (symptomatic and asymptomatic) leaves to follow the time course of fluorescence quenching. Mean values are obtained from the analysis of three different leaves.

Results

Chlorophyll fluorescence imaging reveals a complex, time-varying spatial pattern of the photosynthetic efficiency and NPQ processes in asymptomatic leaves from virus-infected plants. Images of the kinetic pattern of NPQ at 17 d.p.i. in these leaves (Fig. 1) show three well defined areas after 20 sec of the onset of illumination during the fluorescence induction. A sharp dark edge appears marking the border between the surroundings of the main veins and other areas of the mesophyll. During the steady state, the areas surrounded the main veins in virus-infected leaves exhibit a dramatic increase in NPQ levels. NPQ images of the corresponding leaves in healthy plants exhibit a more homogeneous pattern. Kinetics of the PSII quantum yield at the same post-infection time doesn't show such extreme differences between the images from healthy and virus-infected plants. However, a lower PSII efficiency is evident in the stressed plants (data not shown).

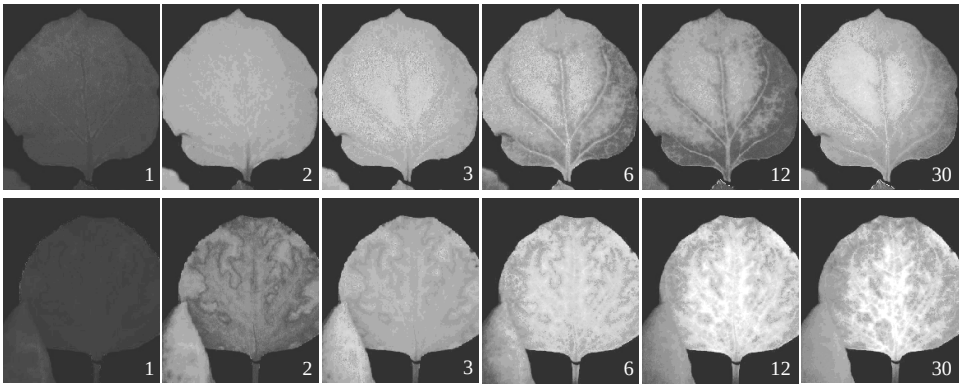

Fig. 1. Imaging of NPQ kinetics at 17 d.p.i. of healthy (A) and asymptomatic leaves of PMMoV infected plants (B)

The time-course of NPQ and Φ_{PSII} was followed at 17 d.p.i. in the above described three different areas of the heterogeneous photosynthetic efficiency pattern of asymptomatic leaves (see Fig. 1). ROIs were selected in the areas surrounding the veins, in the free-vein ones and exactly in the sharp border between both of them, showing a very low NPQ at 20 sec during the fluorescence induction (Fig. 2). These kinetics were compared with those of healthy plants measured in areas close to the veins and in the rest of the leaf. Both areas of control leaves show a similar NPQ and Φ_{PSII} kinetics. However, PSII efficiency was higher in the mesophyll than in areas close to the vascular system. In leaves from infected plants the three mentioned

areas correspond to different levels of energy dissipation, the highest one is surrounding the veins. Differences in Φ_{PSII} efficiency among the three different areas are not so evident.

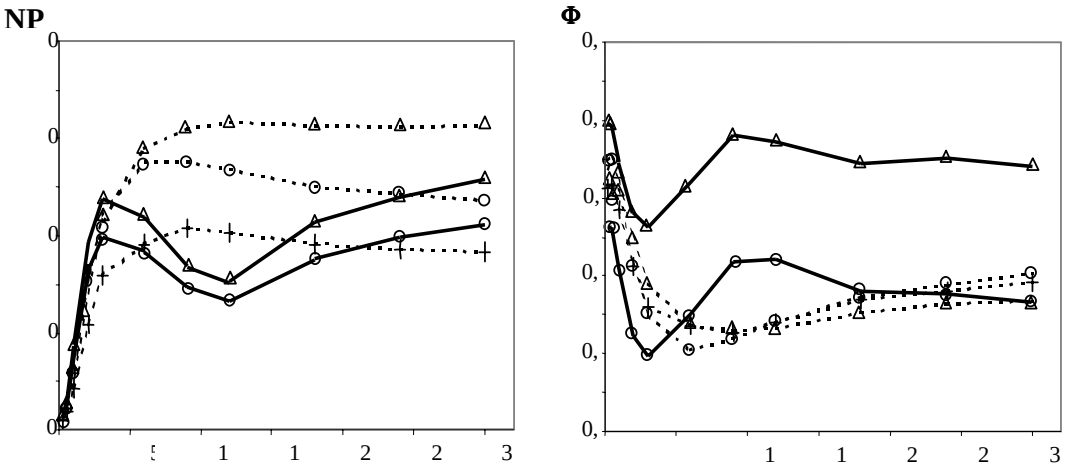

Fig 2. NPQ and Φ_{PSII} time-course measured in healthy (vein and vein-free areas) and asymptomatic leaves of PMMoV-I infected plants (vein , border and vein-free areas) at 17 d.p.i.

The non-photochemical process of energy dissipation seems to be a defence mechanism of PSII against the viral infection. It is composed of multiple processes that include the generation of ph gradient, conformational changes on the photosynthetic apparatus, xanthophyll cycle and the development of photoinhibition. Further work is needed to clarify the involvement of these metabolic processes on the generation of a differential pattern of NPQ in virus-infected plants.

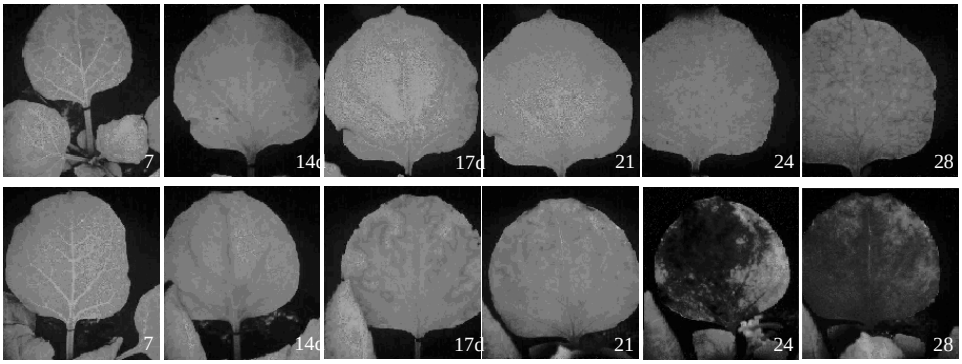

Fig. 3. Imaging of NPQ_{30} at different d.p.i. from healthy (A) and asymptomatic leaves of PMMoV-I infected plants (B)

In Fig. 3 we have also compared NPQ_{30} images (after 30 sec illumination during the fluorescence induction, when the heterogeneity is more evident) of asymptomatic leaves from virus-infected plants, and the corresponding ones of healthy plants at different post-inoculation time. Control leaves show a more homogeneous fluorescence quenching, compared to the heterogeneity of the infected ones. In addition, the dark images of infected

leaves at the last infection stages represent an impaired fluorescence quenching, which could be attributed to dramatic changes in the thylakoid membrane and in the PSII function.

NPQ and Φ_{PSII} images from symptomatic leaves recorded either during the fluorescence induction or along the infection show a homogeneous distribution (data not shown). Curling of these leaves difficults the imaging measurements. From this reason, 4 equivalent ROIs were chosen in a leaf to analyse the mean values of fluorescence quenching kinetics within the leaf at different d.p.i. Similar estimations were made in young leaves of healthy plants.

We have followed the NPQ time-course of symptomatic leaves at different d.p.i. (Fig. 4). Comparing NPQ kinetics obtained in healthy and infected plant at the same post-infection time, they are quite similar mainly at the steady stage. Maximal values of this parameter are exhibited at 60 s after the onset of the illumination at 17 d.p.i. in healthy and infected plants. Time course of the PSII photochemical yield along the infection show minimal values at 28 d.p.i. We have showed previously (Rahoutei *et al*., 2000) that symptomatic leaves exhibit a higher susceptibility to photoinhibition at the last infection stages.

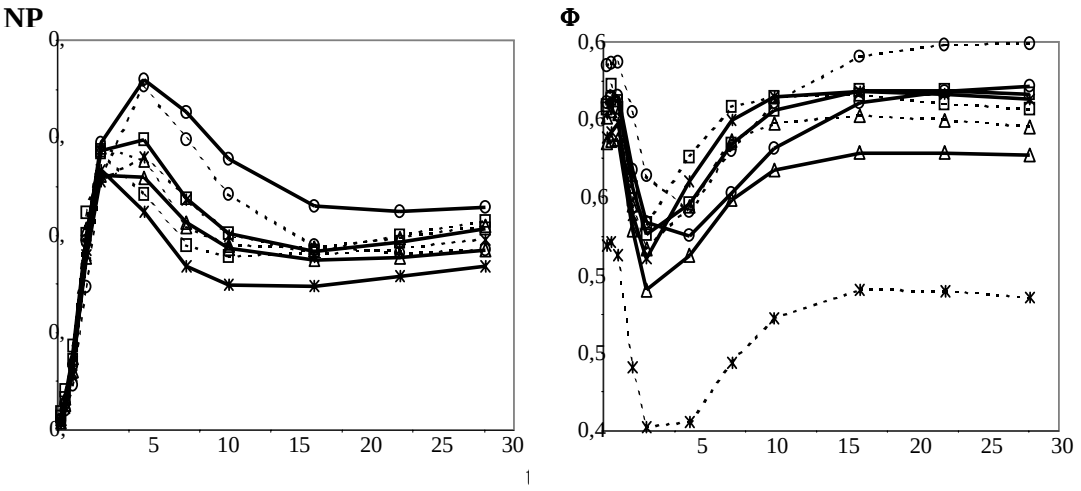

Fig. 4. NPQ and Φ_{PSII} time-course measured in healthy and infected plants at different d.p.i. Control: 7, 14, 17, 28 d.p.i. Symptomatic leaves: 7, 14, 17, 28 d.p.i.

Inhibition of photosynthesis in virus-infected plants is a complex phenomenon, in which photoprotective and inhibitory mechanisms are operating. Fluorescence imaging is a powerful tool to follow these processes along the infection and investigate their heterogeneity within the leaf.

Acknowledgments

This work was supported by grants to M.B. and I.G.L. and a fellowship to M.L.P.B. from the Spanish Ministry of Science and Technology (BIO98-0860-CO2-01 and 02). The Belgian group was financed by BOF Funds of the Slimme Region of the Province of Limburg.

References

Balachandran S, Hurry VM, Kelley SE, Osmond CB, Robinson SA, Rohozinski J, Seaton GGR, and Sims DA (1997). *Physiologia Plantarum* **100**, 203-213.

Ciscato M (2000). Ph. D. Thesis, LUC.

Lichtenthaler HJ (1996). *Plant Physiology* **148**, 4-14.

Peterson RB, Aylor DE (1995). *Plant Physiology* **108**, 163-171.
Rahoutei J, García-Luque I, Barón M (2000) *Physiologia Plantarum* **110**, 286-292.
Scholes JD and Rolfe SA (1996) *Planta* **199**, 573-582.